Supplementary to

Slower growth prior to the 2018 drought and a high growth sensitivity to previous year summer conditions predisposed European beech to crown dieback

Anna Neycken[1], Thomas Wohlgemuth[2], Esther R. Frei[2,3,4], Stefan Klesse[2,5], Andri Baltensweiler[6], Mathieu Lévesque[1]

[1]Silviculture Group, Institute of Terrestrial Ecosystems, ETH Zurich, Universitätsstrasse 16, Zurich 8092, Switzerland

[2]Forest Dynamics, Swiss Federal Institute for Forest, Snow and Landscape Research WSL, Zürcherstrasse 111, 8903 Birmensdorf, Switzerland

[3]Alpine Environment and Natural Hazards, WSL Institute for Snow and Avalanche Research SLF, Flüelastrasse 11, 7260 Davos Dorf, Switzerland

[4]Climate Change and Extremes in Alpine Regions Research Centre CERC, 7260 Davos Dorf, Switzerland

[5]Oeschger Centre for Climate Change Research, University of Bern, Bern, Switzerland

[6]Forest Resources and Management , Swiss Federal Institute for Forest, Snow and Landscape Research WSL, Zürcherstrasse 111, 8903 Birmensdorf, Switzerland

Contact information: anna.neycken@usys.ethz.ch

Table of supplementary tables

Table of supplementary figures

Table of supplementary equations

Supplementary Tables

Table S1. Number and characteristics of the sampled beech trees with crown data in three different regions (Baselland (BL), Zurich/Aargau (ZH/AG) and Schaffhausen (SH)) per year. Only trees that were included in crown-related analyses were considered (22 trees with incomplete data). %CBL is the total crown biomass loss in %. For the vital trees in SH crown data was only available for 2021.

Region	Vitality class	Year	Number of trees	Mean %CBL (range) [%]
Basel (BL)	Early-browning	2020	101	63.1 (19.3 – 100)
	Vital	2020	76	35.2 (0 –85)
Schaffhausen (SH)	Early-browning	2020	107	53.8 (5 – 100)
	Vital	2020	NA	NA
		2021	74	23.6 (15 – 33.5)
Zurich/Aargau (ZH/AG)	Early-browning	2020	48	42.2 (5 – 94)
	Vital	2020	42	17.9 (0 – 64)

Table S2. Summary of the fitted linear mixed effects model that compared the tree-ring width (as log(TRW + 1)) of the three different crown vitality classes (vital, early-browning – minor damage, early-browning – severe damage) from 2016 to 2020 in the region of Basel following Eq. (3). Year was treated as a factor variable to allow for year specific predictions. 2016 is the reference year and "vital" (part A in table) or "early-browning – minor damage" (part B in table) the reference vitality class. In addition, tree ID nested in group was added as grouping variable of the random intercept. The estimate, standard error (std. error) and p-value (p) are given for each term. Significant results are in bold.

Basel	**Estimate**	**Std. error**	**p**
A) Log(tree-ring width + 1), "Vital" as reference			
Intercept	0.745	0.048	**<0.001**
Year [2017]	-0.095	0.031	**0.003**
Year [2018]	0.054	0.032	0.088
Year [2019]	0.039	0.032	0.210
Year [2020]	0.023	0.032	0.461
Vitality [Early-browning – minor damage]	0.021	0.068	0.761
Vitality [Early-browning – severe damage]	-0.092	0.067	0.167
Year [2017] x Vitality [Early-browning – minor damage]	-0.054	0.049	0.264
Year [2018] x Vitality [Early-browning – minor damage]	0.242	0.049	**<0.001**
Year [2019] x Vitality [Early-browning – minor damage]	-0.331	0.049	**<0.001**
Year [2020] x Vitality [Early-browning – minor damage]	-0.040	0.049	0.407
Year [2017] x Vitality [Early-browning – severe damage]	-0.048	0.048	0.315
Year [2018] x Vitality [Early-browning – severe damage]	-0.217	0.048	**<0.001**
Year [2019] x Vitality [Early-browning – severe damage]	-0.336	0.048	**<0.001**
Year [2020] x Vitality [Early-browning – severe damage]	-0.262	0.048	**<0.001**
Observations	845		
Marginal R^2	0.168		
Conditional R^2	0.718		

	Estimate	Std. error	p
B) Log(tree-ring width + 1), "Early-browning – minor damage" as reference			
Intercept	0.766	0.049	**<0.001**
Year [2017]	-0.150	0.037	**<0.001**
Year [2018]	-0.188	0.037	**<0.001**
Year [2019]	-0.292	0.037	**<0.001**
Year [2020]	-0.017	0.037	0.645
Vitality [Vital]	-0.021	0.068	0.761
Vitality [Early-browning – severe damage]	-0.114	0.062	0.069
Year [2017] x Vitality [Vital]	0.054	0.049	0.263
Year [2018] x Vitality [Vital]	0.242	0.049	**<0.001**
Year [2019] x Vitality [Vital]	0.331	0.049	**<0.001**
Year [2020] x Vitality [Vital]	0.040	0.049	0.407
Year [2017] x Vitality [Early-browning – severe damage]	0.006	0.052	0.903
Year [2018] x Vitality [Early-browning – severe damage]	0.025	0.052	0.624
Year [2019] x Vitality [Early-browning – severe damage]	-0.004	0.052	0.931
Year [2020] x Vitality [Early-browning – severe damage]	-0.221	0.052	**<0.001**
Observations	845		
Marginal R^2	0.168		
Conditional R^2	0.718		

Table S3. Summary of the fitted linear mixed effects model that compared the tree-ring width (as log(TRW + 1)) of the three different crown vitality classes (vital, early-browning – minor damage, early-browning – severe damage) from 2016 to 2020 in the region of Zurich/Aargau following Eq. (3). Year was treated as a factor variable to allow for year specific predictions. 2016 is the reference year and "vital" (part A in table) or "early-browning – minor damage" (part B in table) the reference vitality class. In addition, tree ID nested in group was added as grouping variable of the random intercept. The estimate, standard error (std. error) and p-value (p) are given for each term. Significant results are in bold.

Zurich/Aargau	**Estimate**	**Std. error**	**p**
A) Log(tree-ring width + 1), "Vital" as reference			
Intercept	0.957	0.061	**<0.001**
Year [2017]	-0.207	0.038	**<0.001**
Year [2018]	-0.015	0.038	0.702
Year [2019]	0.059	0.038	0.125
Year [2020]	0.040	0.038	0.289
Vitality [Early-browning – minor damage]	-0.241	0.086	**0.009**
Vitality [Early-browning – severe damage]	-0.069	0.112	0.537
Year [2017] x Vitality [Early-browning – minor damage]	0.033	0.055	0.553
Year [2018] x Vitality [Early-browning – minor damage]	-0.190	0.055	**<0.001**
Year [2019] x Vitality [Early-browning – minor damage]	-0.276	0.055	**<0.001**
Year [2020] x Vitality [Early-browning – minor damage]	-0.023	0.055	0.683
Year [2017] x Vitality [Early-browning – severe damage]	-0.057	0.083	0.491
Year [2018] x Vitality [Early-browning – severe damage]	-0.363	0.083	**<0.001**
Year [2019] x Vitality [Early-browning – severe damage]	-0.434	0.083	**<0.001**
Year [2020] x Vitality [Early-browning – severe damage]	-0.220	0.083	**0.008**
Observations	445		
Marginal R^2	0.301		
Conditional R^2	0.759		

	Estimate	Std. error	p
B) Log(tree-ring width + 1), "Early-browning – minor damage" as reference			
Intercept	0.716	0.060	**<0.001**
Year [2017]	-0.174	0.040	**<0.001**
Year [2018]	-0.204	0.040	**<0.001**
Year [2019]	-0.218	0.040	**<0.001**
Year [2020]	0.018	0.040	0.657
Vitality [Vital]	0.241	0.086	**0.009**
Vitality [Early-browning – severe damage]	0.171	0.100	0.074
Year [2017] x Vitality [Vital]	-0.033	0.055	0.553
Year [2018] x Vitality [Vital]	0.190	0.055	**<0.001**
Year [2019] x Vitality [Vital]	0.276	0.055	**<0.001**
Year [2020] x Vitality [Vital]	0.023	0.055	0.683
Year [2017] x Vitality [Early-browning – severe damage]	-0.090	0.084	0.284
Year [2018] x Vitality [Early-browning – severe damage]	-0.173	0.084	**0.039**
Year [2019] x Vitality [Early-browning – severe damage]	-0.158	0.084	0.060
Year [2020] x Vitality [Early-browning – severe damage]	-0.197	0.084	**0.019**
Observations	445		
Marginal R^2	0.301		
Conditional R^2	0.759		

Table S4. Summary of the fitted linear mixed effects model that compared the tree-ring width (as log(TRW + 1)) of the three different crown vitality classes (vital, early-browning – minor damage, early-browning – severe damage) from 2016 to 2020 in the region of Schaffhausen following Eq. (3). Year was treated as a factor variable to allow for year specific predictions. 2016 is the reference year and "vital" (part A in table) or "early-browning – minor damage" (part B in table) the reference vitality class. In addition, tree ID nested in group was added as grouping variable of the random intercept. The estimate, standard error (std. error) and p-value (p) are given for each term. Significant results are in bold.

Schaffhausen	**Estimate**	**Std. error**	**p**
A) Log(tree-ring width + 1), "Vital" as reference			
Intercept	0.921	0.043	**<0.001**
Year [2017]	-0.279	0.030	**<0.001**
Year [2018]	-0.157	0.030	**<0.001**
Year [2019]	-0.037	0.030	0.210
Year [2020]	0.033	0.030	0.270
Vitality [Early-browning – minor damage]	-0.135	0.058	**0.022**
Vitality [Early-browning – severe damage]	-0.254	0.064	**<0.001**
Year [2017] x Vitality [Early-browning – minor damage]	-0.042	0.043	0.328
Year [2018] x Vitality [Early-browning – minor damage]	-0.214	0.043	**<0.001**
Year [2019] x Vitality [Early-browning – minor damage]	-0.262	0.043	**<0.001**
Year [2020] x Vitality [Early-browning – minor damage]	-0.146	0.043	**<0.001**
Year [2017] x Vitality [Early-browning – severe damage]	0.031	0.050	0.535
Year [2018] x Vitality [Early-browning – severe damage]	-0.113	0.050	**0.025**
Year [2019] x Vitality [Early-browning – severe damage]	-0.265	0.050	**<0.001**
Year [2020] x Vitality [Early-browning – severe damage]	-0.289	0.050	**<0.001**
Observations	905		
Marginal R^2	0.341		
Conditional R^2	0.725		

	Estimate	Std. error	p
B) Log(tree-ring width + 1), "Early-browning – minor damage" as reference			
Intercept	0.786	0.039	**<0.001**
Year [2017]	0.321	0.031	**<0.001**
Year [2018]	-0.371	0.031	**<0.001**
Year [2019]	-0.299	0.031	**<0.001**
Year [2020]	-0.113	0.031	**<0.001**
Vitality [Vital]	0.135	0.058	**0.022**
Vitality [Early-browning – severe damage]	-0.119	0.054	**0.027**
Year [2017] x Vitality [Vital]	0.042	0.043	0.328
Year [2018] x Vitality [Vital]	0.214	0.043	**<0.001**
Year [2019] x Vitality [Vital]	0.262	0.043	**<0.001**
Year [2020] x Vitality [Vital]	0.146	0.043	**<0.001**
Year [2017] x Vitality [Early-browning – severe damage]	0.073	0.051	0.151
Year [2018] x Vitality [Early-browning – severe damage]	0.101	0.051	**0.049**
Year [2019] x Vitality [Early-browning – severe damage]	-0.004	0.051	0.942
Year [2020] x Vitality [Early-browning – severe damage]	-0.143	0.051	**0.006**
Observations	905		
Marginal R^2	0.341		
Conditional R^2	0.725		

Supplementary Figures

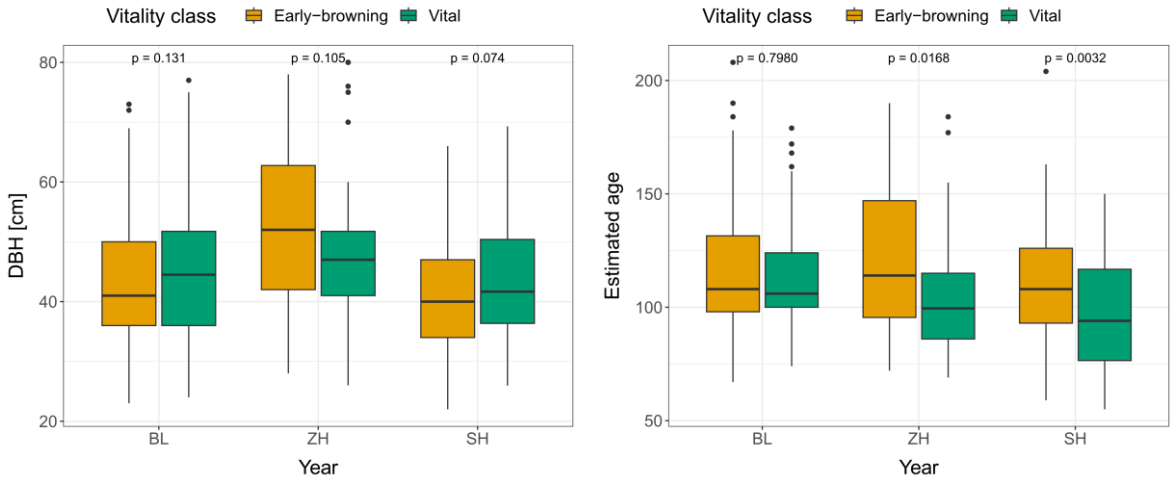

Figure S1. Differences in diameter at breast height (DBH, left) and estimated age (right) between vital (green) and early-browning (orange) trees for each region (BL, ZH/AG, SH) separately. The differences between the vitality classes were tested using Wilcoxon rank sum test ($\alpha < 0.05$). The age could be only estimated for 455 out of 470 trees. The mean difference between the age estimates of the two increment cores per tree was 10 years.

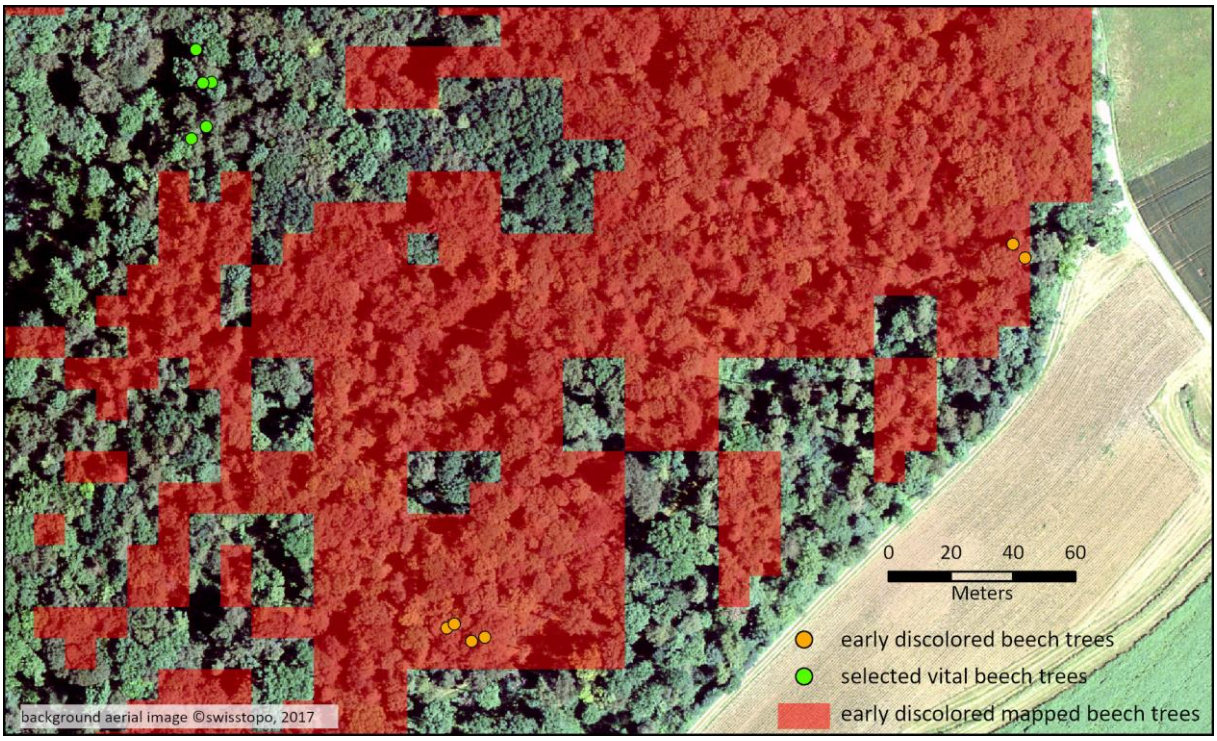

Figure S2. Example of vital beech trees selection in the region of Schaffhausen close to previously observed early-browning beech trees (orange dots) with no early browning between 25th of August 2018 and the 20th of September 2018 (green dots). The pixels (10 m resolution) in which remote sensing detected early browning are given in red. To map beech trees with early browning across Switzerland, we utilized Sentinel-2 satellite images. Vegetation indices (VIs) were derived for 2018, 2017, and 2016 (Baltensweiler, 2020). To compare with previous years, we calculated VIs (specifically NDVI (normalized difference vegetation index) and NDWI (normalized difference water index)) at various time intervals between June and September 2018 and compared them to the corresponding periods in 2016 and 2017. Significant decreases in VI from 2018 to previous years indicated the occurrence of early browning. By extracting the VI data at the locations of the 963 observed vital and early discolored beech trees published in Frei et al. (2022), we established a threshold and subsequently classified the trees as either vital or affected by drought in the Swiss forest. This classification process was limited to areas delineated by a beech distribution map (Wüest et al., 2021) and high-resolution classification of tree types (broadleaved/coniferous) (Waser et al., 2017).

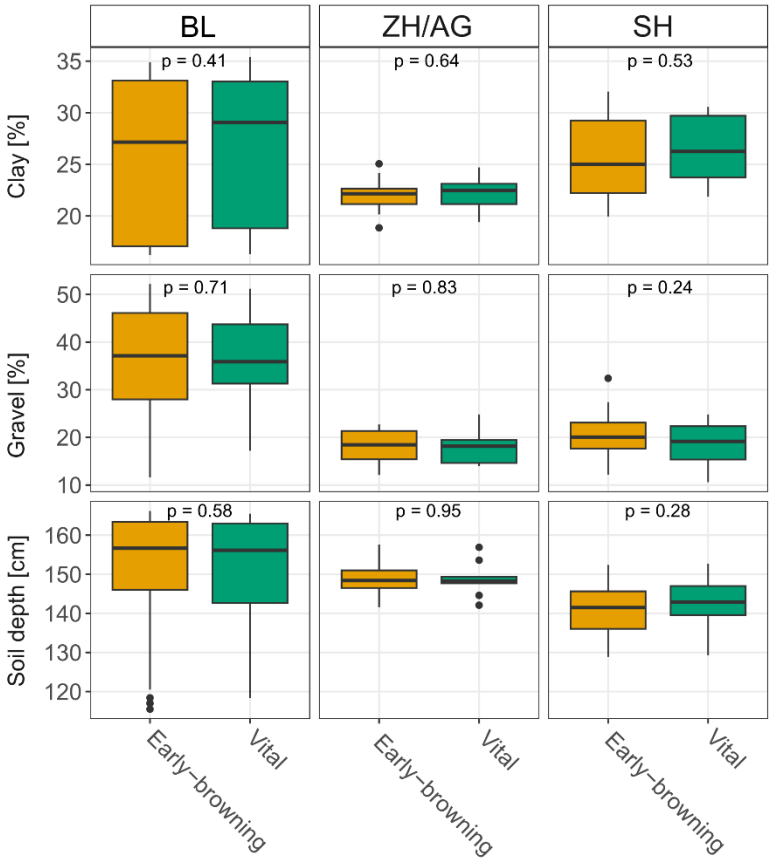

Figure S3. Modeled soil parameters (clay content, gravel content, soil depth) per tree group and region (BL, ZH/AG, SH). The data was extracted for each tree group from machine-learning based soil maps for forested areas in Switzerland (Baltensweiler et al., 2021, www.wsl.ch/soilmaps/). The model predicts soil data on a 25x25 m grid. Differences between vital and early-browning tree groups were tested separately for each region and soil parameter using a Wilcoxon rank sum test ($\alpha < 0.05$).

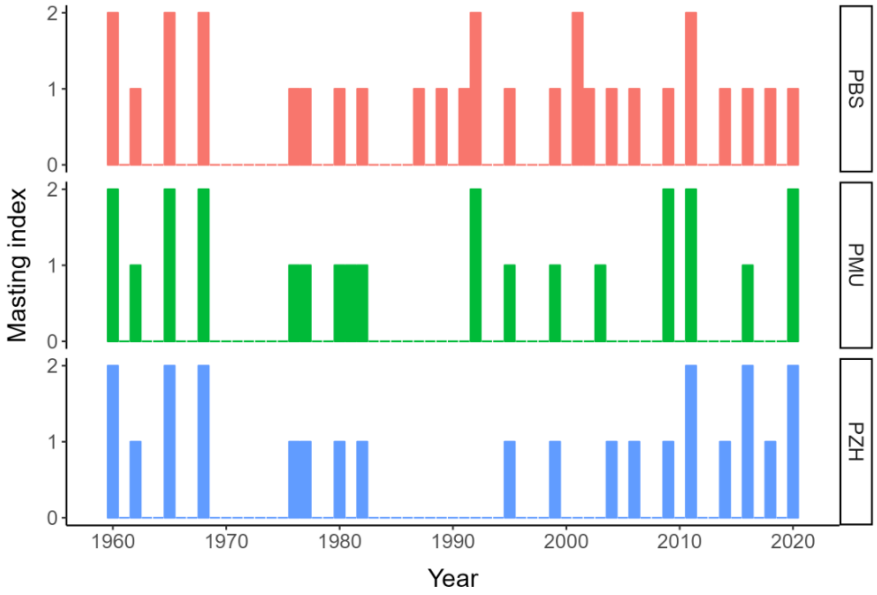

Figure S4. Masting index based on beech pollen data from three MeteoSwiss weather stations between 1969 and 2020 (Swiss Federal Office of Meteorology and Climatology, PBS (Basel, 7°35'/47°34'), PMU (Münsterlingen, 9°14'/47°38') and PZH (Zurich, 8°34'/47°23'), Fig. S5), seed data from the region of Baden-Württemberg (Germany) for the time window 1961–1968 (Ascoli et al., 2017) and beech mast data from Switzerland from Jenni (1987) for the year 1960. The masting likelihood was estimated on an ordinal scale with three levels: 0 – low likelihood, 1 – medium likelihood, 2 - high likelihood.

The masting index was calculated as follows. First, we calculated the yearly pollen concentration for each tree group based on the available daily beech pollen count data collected by MeteoSwiss weather stations (Swiss Federal Office of Meteorology and Climatology) closest to the groups. The pollen count data was available for the period 1969–2020 for the station Basel (7°35'/47°34'), for 1981 – 2020 for the station Zürich (8°34'/47°23') and for 1987–2020 for the station Münsterlingen (9°14'/47°38'). The masting index was calculated by grouping the yearly pollen concentrations of each station into three different classes assuming that pollen concentration can be used as a bioindicator for masting (Kasprzyk et al., 2014). The highest one-third of the yearly pollen concentrations per station received a score of 2, while the lowest third received a score of 0 and average pollen concentration a score of 1. The pollen concentration data from the station Basel was used to complete the missing data for the other two stations (Fig. S5). Second, masting data based on

field observations conducted in Baden-Württemberg (Germany) by the “Staatsklenge Forstamt Nagold” (Ascoli et al., 2017) spanning the period 1961–1968 were used. The original ordinal masting scale ranged from 1 to 5, with 1 signifying no or very low masting, and 5 full mast. We homogenized the scale of these two data sets by rescaling the data so that 1 was converted to 0; 2 and 3 became 1; and 4 and 5 were converted to 2. Third, Jenni (1987) reported a full mast for beech in Switzerland in 1960, which was included in the masting index with the value 2.

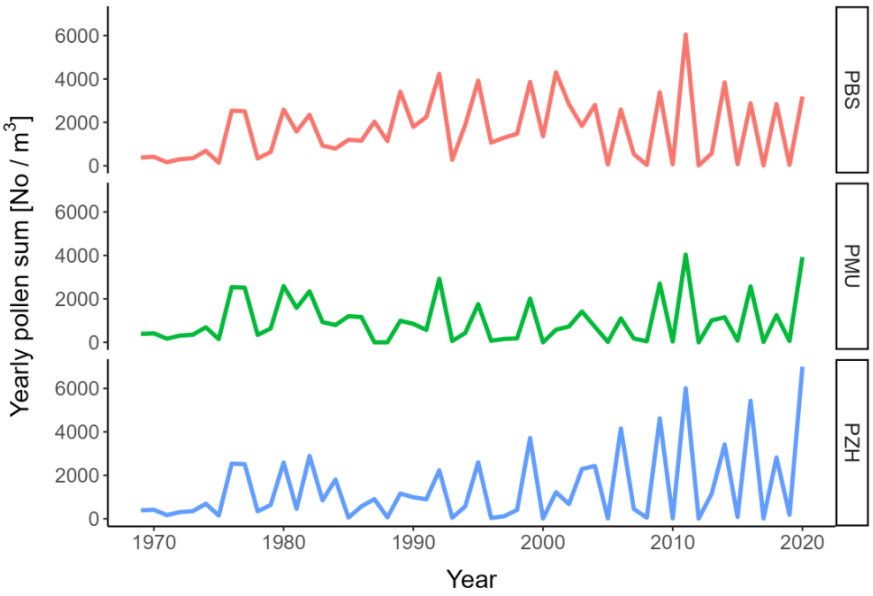

Figure S5. Yearly pollen concentration (given as the sum of yearly measured pollen amount per m^3 air) for beech measured at three different MeteoSwiss weather stations (Swiss Federal Office of Meteorology and Climatology): Basel (PBS, 7°35'/47°34'), Münsterlingen (PMU, 9°14'/47°38') and Zurich (PZH, 8°34'/47°23'). Because the data for PMU was only available between 1987 – 2020 and for PZH between 1981–2020, the data from PBS (data for 1969–2020) was used to fill the gaps.

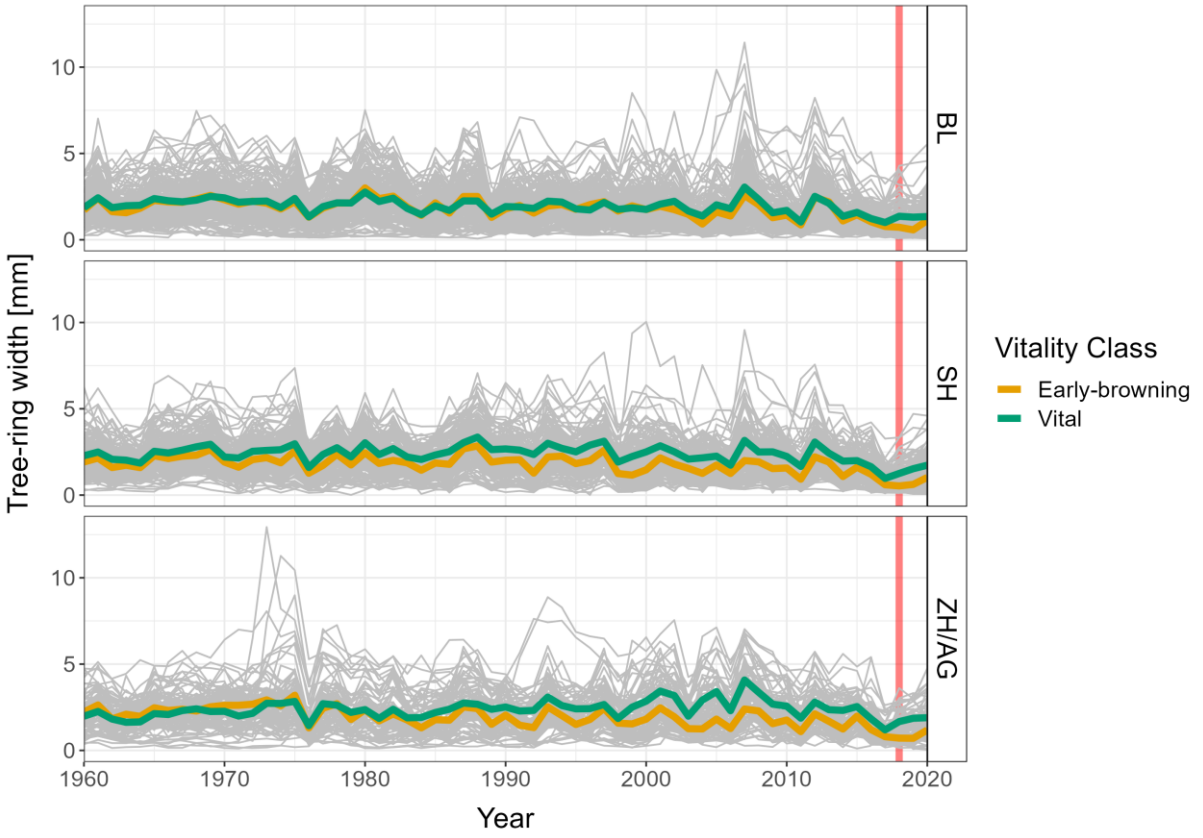

Figure S6. Raw individual tree tree-ring width chronologies (gray lines) plotted separately for the three investigated regions: BL, ZH/AG and SH. Mean tree-ring width for vital (green lines) and early-browning (orange lines) beech trees are shown per study region. The red vertical line highlights the year 2018.

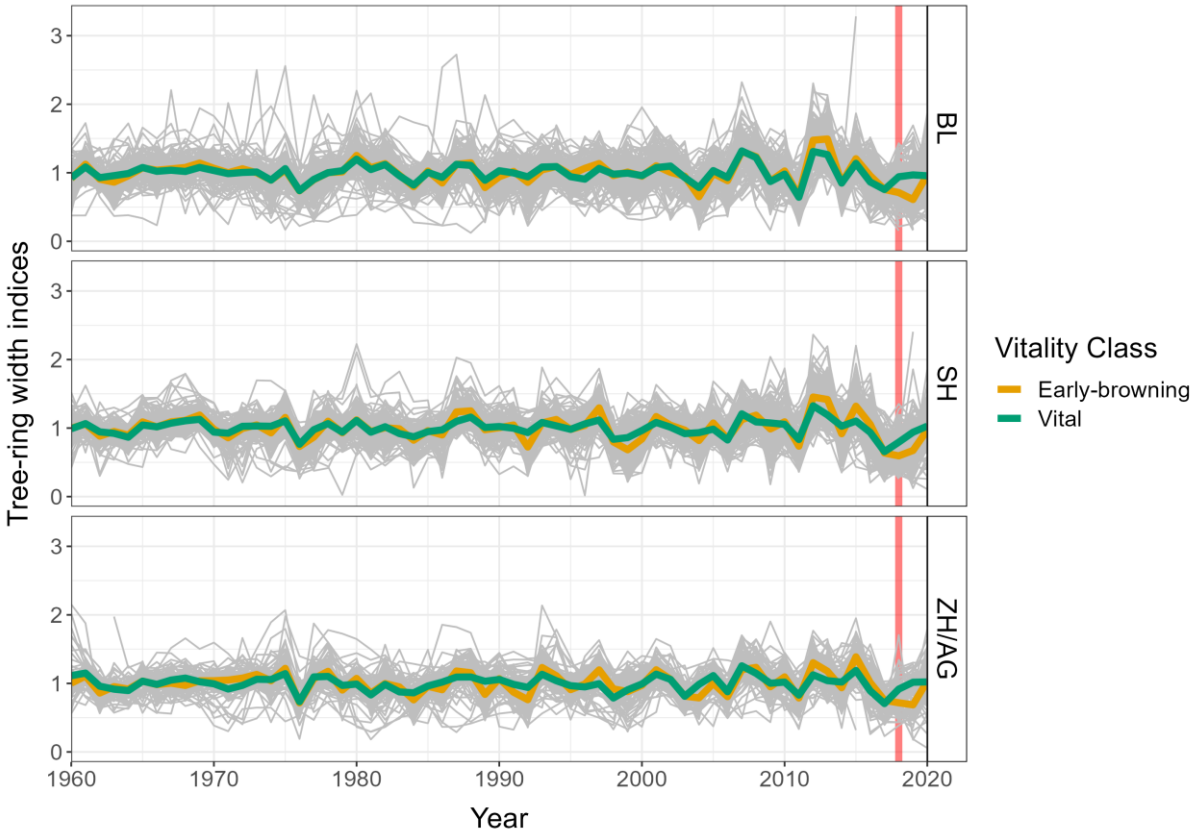

Figure S7. Individual tree-ring width index series (gray lines) plotted separately for the three investigated regions: BL, ZH/AG and SH. The raw tree-ring width series were detrended following Eq. (S1). Mean tree-ring width index for vital (green lines) and early-browning (orange lines) beech trees are shown per study region. The red vertical line highlights the year 2018.

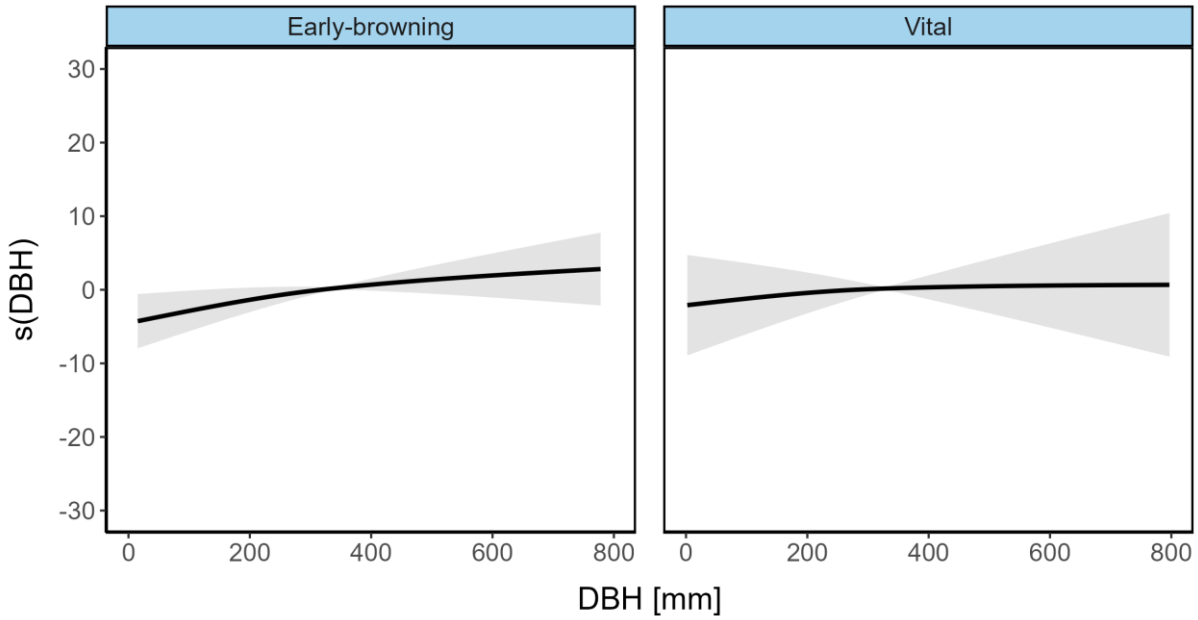

Figure S8. Population-wide smooth function for the partial effect of the diameter at breast height (DBH) corresponding to term $f_1(DBH_{ig})$ in Eq. (2) for vital and early-browning trees. The effect was modeled by a cubic regression spline. The y-axis gives the value of the centered smooth (s(DBH)). Thus, it is the contribution of the smooth function to the fitted value. The confidence intervals are given as grey shaded areas.

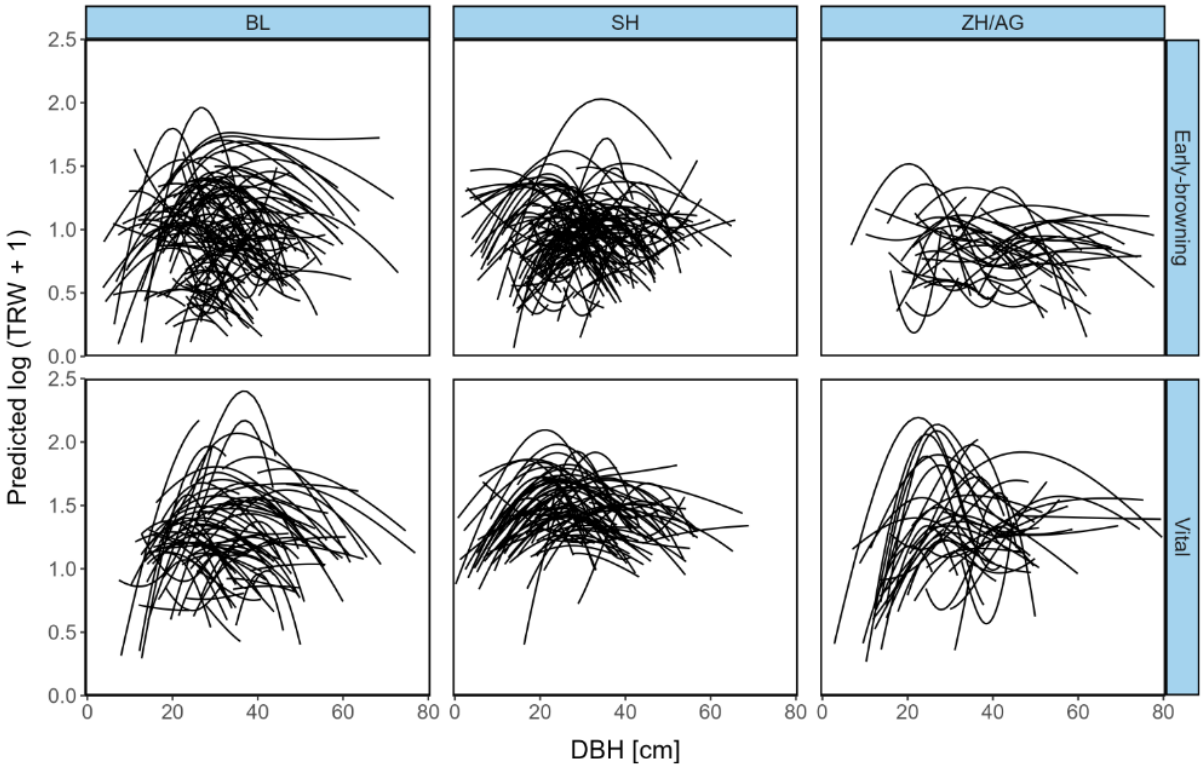

Figure S9. Predicted log +1 transformed tree-ring width (TRW) in function to diameter at breast height (DBH) for each individual tree (black lines) grouped by region: Baselland (BL), Schaffhausen (SH) and Zurich/Aargau (ZH/AG) and vitality class (vital or early-browning). The values were predicted while setting the climate terms to the mean and the masting index to 0.

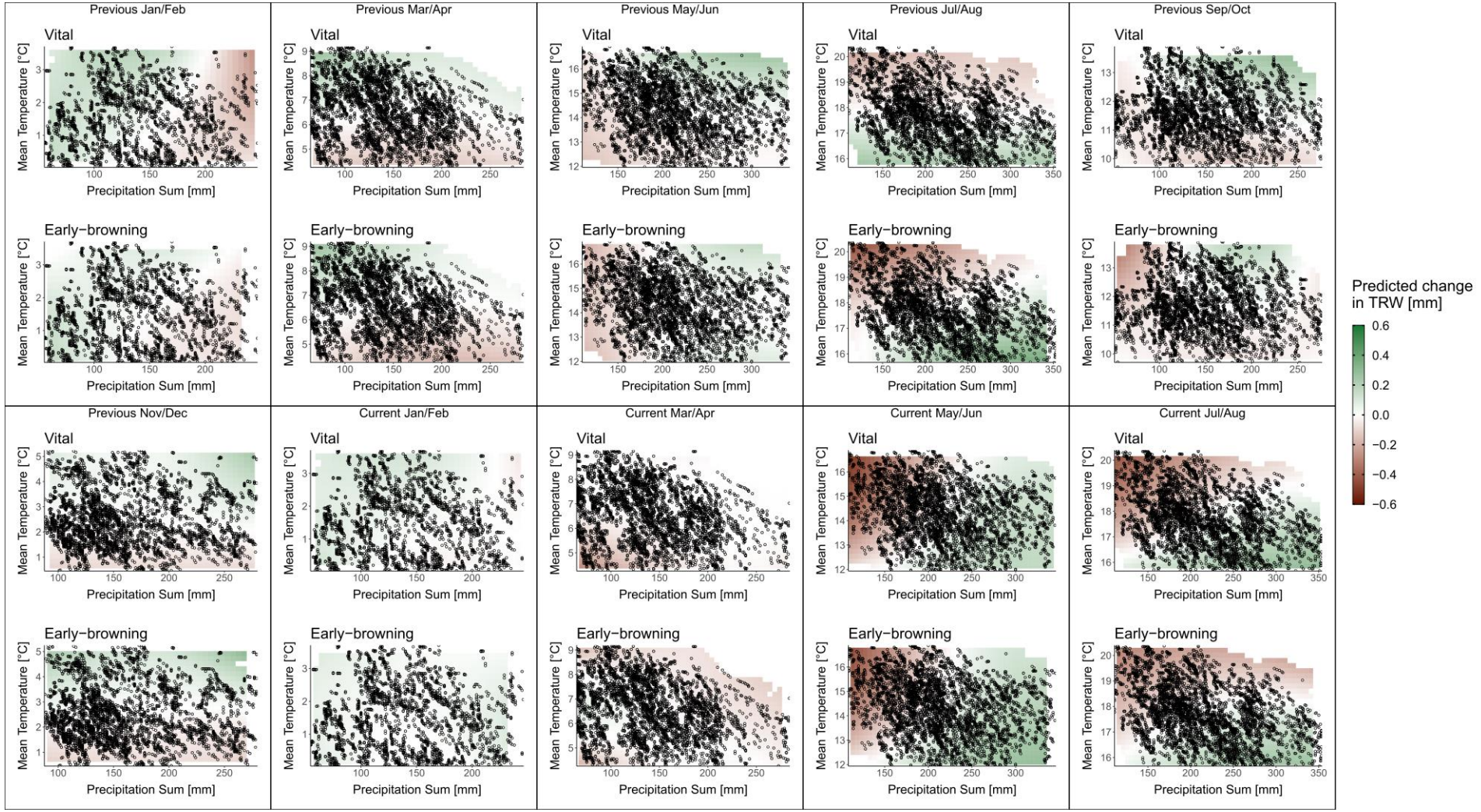

Figure S10: Predicted change in tree-ring width (TRW) of vital and early-browning beech trees in function of mean temperature and precipitation sum of the previous and current year for two-months periods from previous year January to current year August following Eq. (S6 & S7) and calculated

for the period 1960–2017. The months are abbreviated by the first three letters. Brown signifies narrower TRW values compared to mean conditions and green indicates larger TRW values. The black circles give the raw data points used for the predictions.

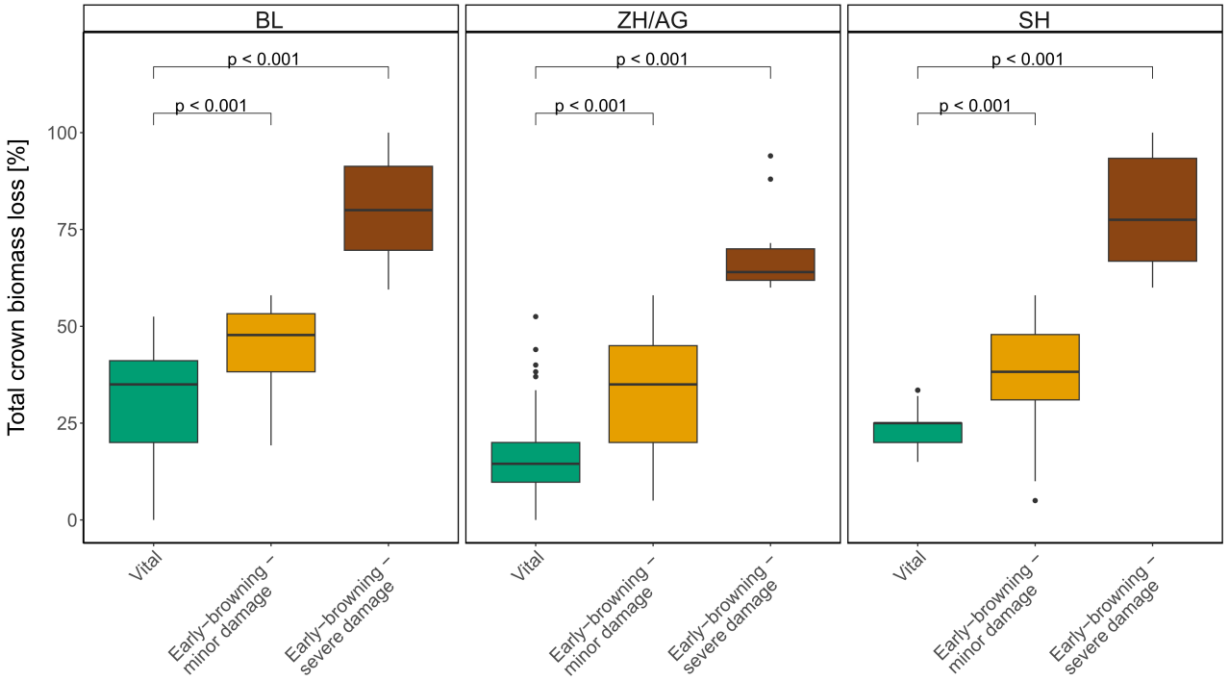

Figure S11. Difference in total crown biomass loss observed in 2020 between the three vitality classes (vital, early-browning – minor damage, early-browning – severe damage) per region (Basel (BL), Zurich/Aargau (ZH/AG), Schaffhausen (SH)). %CBL is the total crown biomass loss percentage observed in 2020. Early-browning trees that had %CBL > 58% were categorized as “severe damage”, trees with %CBL ≤ 58% minor damage”. The p-values displayed over the boxplots are the results of a Wilcoxon rank sum test ($\alpha < 0.05$).

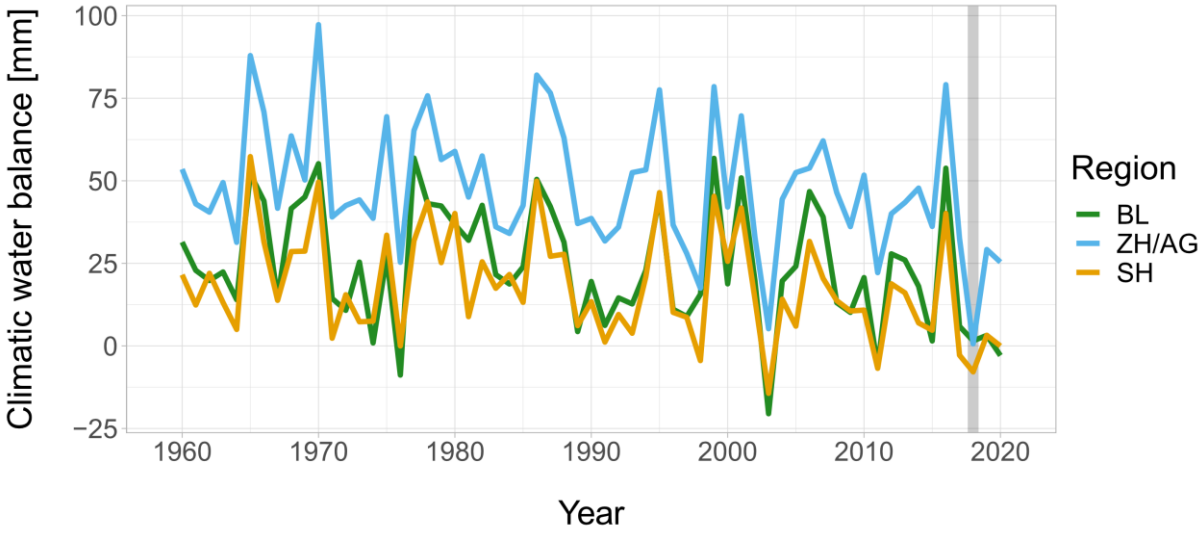

Figure S12. Average Climatic water balance (CWB) for the period January–August calculated separately for the three different regions (Basel (BL, green), Zurich/Aargau (ZH/AG, blue), Schaffhausen (SH, orange)) between 1960 and 2020. The gray vertical line highlights 2018. CWB was calculated by subtracting the monthly potential evapotranspiration (Thornthwaite, 1948) from the monthly precipitations sum.

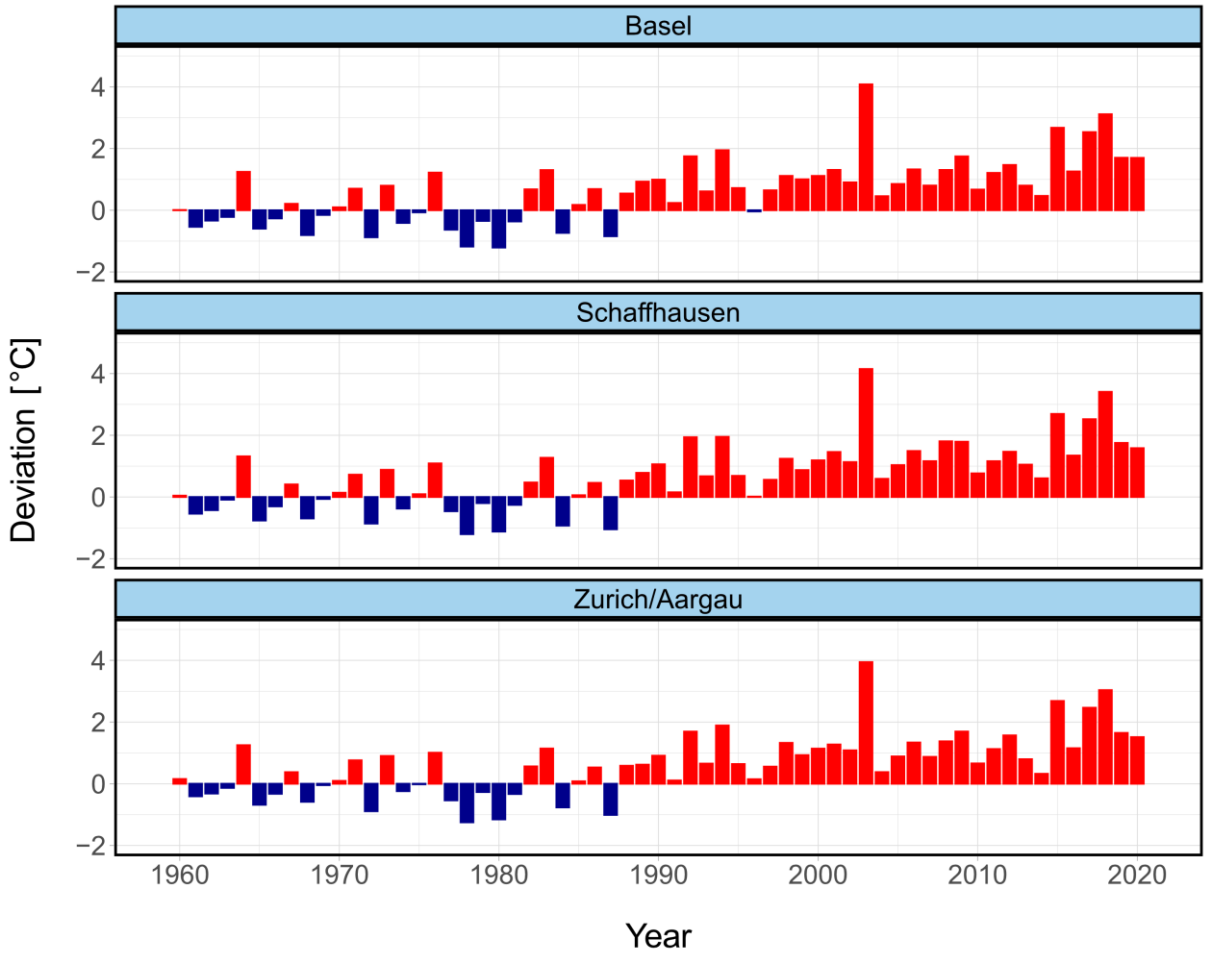

Figure S13. Temperature anomalies of the months May to August calculated from 1960 to 2020 for each region separately. Red bars indicate years with higher and blue bars lower mean temperatures compared to the reference period 1960–1990.

Supplementary Equations

Equations S1 & S2. We calculated the standard deviation and the first order autoregressive coefficient (AR1) of the detrended tree-ring width series (TRW) as follows according to Venables and Ripley (2002):

$$Standard\ deviation = \sqrt{\frac{\sum|x_t - \bar{x}|^2}{n}}$$

$$AR_k = \frac{\sum_{t=k+1}^{n}(x_t - \bar{x})(x_{t-k} - \bar{x})}{\sum_{t=1}^{n}(x_t - \bar{x})^2}, with\ k = 1$$

x_t is the time series (in our case TRW), $\bar{x}$ is the mean of the timeseries, n the number of observations and x_{t-k} the timeseries shifted by k units (for AR1 k =1). The formula for AR1 further assumes second-order stationarity of the time series.

Equations S3 & S4. We used an additive model (Wood, 2017) to detrend tree individual tree-ring width chronologies along reconstructed DBH (diameter at breast height). The model was run for each tree separately between 1960 and 2020. DBH was modeled as a flexible cubic regression spline with a maximum of six degrees of freedom and restricted maximum likelihood (REML) as the smoothing parameter estimation method. The model was formulated as follows:

$$\log(TRW_{it} + 1) = f(DBH_{it}) + \varepsilon_{it}$$

where TRW_{it} is the tree-ring width of tree *i* in year *t* and DBH_{it} is the diameter at breast height of tree *i* in year *t*. The formulation of the R-code using the R-package *mgcv* (v1.8-40, Wood, 2011) was:

```
gam(log(TRW +1) ~ s(DBH, k = 6, bs = "cr"),
     method = "REML", family = "gaussian",
     data = data)
```

`log(TRW +1)` gives the log + 1 transformed TRW. The transformation was applied to achieve the normal distribution of the residuals. `s(DBH, k = 6, bs = "cr")` describes the cubic regression spline (`bs = "cr"`) with a maximum of six degrees of freedom (`k = 6`) for the tree individual size trend. The model was fitted with a gaussian distribution (`family = "gaussian)`.

Equation S5.

$$Parameter_{ij} = \beta_0 + \beta_1 \text{vitality}_{\,i} + \beta_2 DBH_{2018,i} + u_j + \varepsilon_{ij}$$

where $Parameter_{ij}$ is either the mean raw TRW for 1960–2017, the linear regression coefficient of raw TRW of 1960–2017, growth variability of the period 1960–2017 or AR1 for the period 1960–2017 of tree *i* in group *j,* $\text{vitality}_{\,i}$ indicates the vitality class of each tree *i*, $DBH_{2018,i}$ is the diameter at breast height in the year 2018 of each tree *i*, u_j is the random intercept for tree group *j*, and ε_{ij} indicates the error term. Growth standard deviation was log-transformed to achieve normal distributed residuals.

Equation S6 & S7. The distributed time lag models were built from three main components: a) a first part describing the size-dependent long-term growth trend for the whole set of study trees and each individual tree, which can be understood as a "model internal detrending" of each TRW series along its own reconstructed DBH time series; b) a second part relating the effect of variabilities in temperature and precipitation, and their interaction over the different lags on raw TRW; and c) a third part including the masting index. We used the flexible penalized spline formulation of the *bam* function from the *mgcv* package (v 1.8-40, Wood, 2011) to model the effects of DBH and climate on growth response. For each vitality class, a separate model was formulated as follows:

$$\log(TRW_{ig} + 1)$$

$$= f_1(DBH_{ig}) + f_2(DBH_{ig})ID_{ig} + \sum_{k=1}^{10} f_3\left(Tmean_{igk}, lag_{igk}\right)$$

$$+ \sum_{k=1}^{10} f_4(PrecSum_{igk}, lag_{igk})$$

$$+ \sum_{k=1}^{10} f_5(Tmean_{igk}, PrecSum_{igk}, lag_{igk}) + Masting_{ig} + f_6(ID_{ig})$$

$$+ f_7(Group_g) + \varepsilon_{ig}$$

$$\text{with } lag_{igk} = (k-1)$$

where $\log(TRW_{ig} + 1)$ is the log + 1 transformed TRW of tree *i* in group *g*. $f_1(DBH_{ig})$ describes a smoother which characterizes a common (population) growth trend over increasing DBH (size trend). This size trend is shared by all *i* trees in groups *g* of the model. Because each tree might have its own size trend which deviates from the common trend, $f_2(DBH_{ig})ID_{ig}$ allows for an additional separate DBH smoother for each tree *i* in group *g*. The third, fourth and fifth sum terms in the formula describe the distributed time lag model. Term $\sum_{k=1}^{10} f_3\left(Tmean_{igk}, lag_{igk}\right)$ models the effect of the temperature measured for tree *i* in group *g* during $lag_{igk} = (k-1)$ as smooth surface, while $\sum_{k=1}^{10} f_4(PrecSum_{igk}, lag_{igk})$ does the same for precipitation. The maximum number of lags (10) is set by the number of time periods investigated. To also consider the interaction between temperature and precipitation in each lag, the tensor product $\sum_{k=1}^{10} f_5(Tmean_{igk}, PrecSum_{igk}, lag_{igk})$ was added to the model. $Masting_{ig}$ is the masting index for tree *i* in group *g* for the current year. This term was considered as parametric term without smoother. $f_6(ID_{ig})$ and $f_7(Group_g)$ give the random intercepts for tree individual *i* and tree group *g*. Last, ε_{ig} gives the common error term which is normally distributed. All variables were scaled to mean 0 and variance 1 before modeling.

The advantage of this method is that no a priori assumption of strict linearity of the effects is made. Moreover, the model penalizes overly wiggly smooths and thereby reduces overfitting.

The model was fitted separately for vital and early-browning trees because no possibility to include a *by-factor interaction* into a matrix argument exists. The by-factor interaction would allow to fit two separate smooths per vitality class (see for example Neycken et al., 2022). The matrix formulation of the predictors is necessary so that multiple lagged temperatures and precipitation sums can be computed by the model at the same time.

The two models were run with the *bam* function from the *mgcv* package (v 1.8-40, Wood, 2011) in R 4.2.1 (R Core Team, 2022) with the following code:

```
bam(log(TRW + 1) ~ s(DBH, bs = "cr", m = 2, k = 4) +
                   s(DBH, by = ID, bs = "cr", m = 1, k = 4) +
                   te(Tmean, lag, k = c(3, 10)) +
                   te(PrecSum, lag, k = c(3, 10)) +
                   te(Tmean, PrecSum, lag, k = c(3, 3, 10)) +
                   s(group, bs = "re") +
                   s(ID, bs = "re") +
                   Masting_index,
                   family = "gaussian",
                   method = "fREML",
                   data = data)
```

`Log(TRW + 1)` indicates that TRW was log-transformed and 1 was added to achieve normality of the residuals. This allowed us to run the model under gaussian assumptions (`family = "gaussian"`) which decreased computation time significantly compared to a generalized additive model (GAM, Wood, 2017). `s(DBH, bs = "cr", m = 2, k = 4)` describes the population-wide size trend along DBH (diameter at breast height) and `s(DBH, by = ID, bs = "cr", m = 1, k = 4)` the tree individual (defined through the tree ID) deviation from the common size trend. The smooths were fitted with cubic regression splines (`bs = "cr"`) which are more computational efficient compared to the standard thin-plate splines. Moreover, we set the marginal basis penalization to the squared second derivative of the function (`m = 2`) for the population-smooth and to the first derivative for the individual smooth (`m = 1`). This setup reduces the collinearity between the population-smooth and the individual ones (Pedersen et al., 2019). In addition, the maximum number of degrees of freedom was restricted to 4 (`k = 4`) because we wanted to retain the high-frequency growth changes.

To model the distributed time lag model with the climatic parameters we used tensor product smooths (`te()`). These smooths are used to define the interactions between temperature, precipitation, and the lags. Each of the parameters is set up as a matrix which includes one column per lag. The maximum amount of freedom was set to 3 for the climate parameters and to 10 for the lag matrix (because 10 lags were included in the analysis).

Next, `s(group, bs = "re")` and `s(ID, bs = "re")` define random intercepts for ID (tree individual) and tree group. This is necessary to account for the sampling design and add the growth level for each tree (Pedersen et al., 2019). Last, the masting index was added to the model as continuous parametric term without smoothing parameter. The model computation method was left at the default which is fast REML (`fREML`, Wood et al., 2015).

Equation S8.

$$\log(TRW + 1)_{ijt} = \beta_0 + \beta_1 year_t + \beta_2 vitality_i + \beta_3 year_t \times vitality_i + b_i + u_{ij} + \varepsilon_{ijt}$$

where $\log(TRW + 1)_{ijt}$ is the log + 1 transformed TRW of tree *i* in group *j* in year *t*, $vitality_i$ is the vitality class of each tree *i*, b_i and u_{ij} are the grouping variables for the random intercept of tree ID nested in tree group, finally ε_{ijt} gives the error term. The model was fitted separately for each region with REML.

References

Ascoli, D., Maringer, J., Hacket-Pain, A., Conedera, M., Drobyshev, I., Motta, R., Cirolli, M., Kantorowicz, W., Zang, C., Schueler, S., Croisé, L., Piussi, P., Berretti, R., Palaghianu, C., Westergren, M., Lageard, J.G.A., Burkart, A., Gehrig Bichsel, R., Thomas, P.A., Beudert, B., Övergaard, R., Vacchiano, G., 2017. Two centuries of masting data for European beech and Norway spruce across the European continent. Ecology 98, 1473–1473. https://doi.org/10.1002/ecy.1785

Baltensweiler, 2020. Räumliche Analyse von Trockenheitssymptomen im Schweizer Wald mit Sentinel-2-Satellitendaten. Schweizerische Zeitschrift für Forstwesen 171, 298–309. https://doi.org/10.3188/szf.2020.0298

Baltensweiler, A., Walthert, L., Hanewinkel, M., Zimmermann, S., Nussbaum, M., 2021. Machine learning based soil maps for a wide range of soil properties for the forested area of Switzerland. Geoderma Regional 27, e00437. https://doi.org/10.1016/j.geodrs.2021.e00437

Frei, E.R., Gossner, M.M., Vitasse, Y., Queloz, V., Dubach, V., Gessler, A., Ginzler, C., Hagedorn, F., Meusburger, K., Moor, M., Samblás Vives, E., Rigling, A., Uitentuis, I., von Arx, G., Wohlgemuth, T., 2022. European beech dieback after premature leaf senescence during the 2018 drought in northern Switzerland. Plant Biol J 24, 1132–1145. https://doi.org/10.1111/plb.13467

Jenni, L., 1987. Mass Concentrations of Bramblings Fringilla montifringilla in Europe 1900-1983: Their Dependence upon Beech Mast and the Effect of Snow-Cover. Ornis Scandinavica 18, 84. https://doi.org/10.2307/3676843

Kasprzyk, I., Ortyl, B., Dulska-Jeż, A., 2014. Relationships among weather parameters, airborne pollen and seed crops of Fagus and Quercus in Poland. Agricultural and Forest Meteorology 197, 111–122. https://doi.org/10.1016/j.agrformet.2014.05.015

Neycken, A., Scheggia, M., Bigler, C., Lévesque, M., 2022. Long-term growth decline precedes sudden crown dieback of European beech. Agricultural and Forest Meteorology 324, 109103. https://doi.org/10.1016/j.agrformet.2022.109103

Pedersen, E.J., Miller, D.L., Simpson, G.L., Ross, N., 2019. Hierarchical generalized additive models in ecology: an introduction with mgcv. PeerJ 7, e6876. https://doi.org/10.7717/peerj.6876

R Core Team, 2022. R: A language and environment for statistical computing. R Foundation for Statistical Computing, Vienna, Austria.

Thornthwaite, C.W., 1948. An Approach toward a Rational Classification of Climate. Geographical Review 38, 55–94. https://doi.org/10.2307/210739

Venables, W.N., Ripley, B.D., 2002. Modern Applied Statistics with S, Statistics and Computing. Springer New York, New York, NY. https://doi.org/10.1007/978-0-387-21706-2

Waser, L., Ginzler, C., Rehush, N., 2017. Wall-to-Wall Tree Type Mapping from Countrywide Airborne Remote Sensing Surveys. Remote Sensing 9, 766. https://doi.org/10.3390/rs9080766

Wood, S.N., 2017. Generalized additive models: an introduction with R, 2nd ed. CRC press.

Wood, S.N., 2011. Fast stable restricted maximum likelihood and marginal likelihood estimation of semiparametric generalized linear models: Estimation of Semiparametric Generalized Linear Models. Journal of the Royal Statistical Society: Series B (Statistical Methodology) 73, 3–36. https://doi.org/10.1111/j.1467-9868.2010.00749.x

Wood, S.N., Goude, Y., Shaw, S., 2015. Generalized Additive Models for Large Data Sets. Journal of the Royal Statistical Society Series C: Applied Statistics 64, 139–155. https://doi.org/10.1111/rssc.12068

Wüest, R.O., Bergamini, A., Bollmann, K., Brändli, U.-B., Baltensweiler, A., 2021. Modellierte Verbreitungskarten für die häufigsten Gehölzarten der Schweiz. Schweizerische Zeitschrift fur Forstwesen 172, 226–233. https://doi.org/10.3188/szf.2021.0226